INSTITUTO SUPERIOR TÉCNICO

UNIVERSIDADE DE LISBOA

PROJETO INTEGRADOR DE 1º CICLO

Single-stage optimization of nuclear fusion devices

Author:
João RODRIGUES

Supervisor:
Prof. Rogério JORGE

Research work performed for the Bachelor degree in Engineering Physics

at

Instituto de Plasmas e Fusão Nuclear
Physics Department

June 15, 2023

Abstract

The potential of nuclear fusion as an option for the production of clean energy prompts the need for plasma confinement devices. Addressing this need, this work focuses on fusion devices of the stellarator type. Historically, this device has been computationally optimized using a two stage approach that independently finds a target magnetic field that confines the plasma and then finds a set of electromagnetic coils that recreate such field. However, the second step is an ill-posed problem which can lead to insurmountable engineering challenges. In this work, a novel single-stage approach is considered, where the traditional two steps are performed simultaneously with multiple iterations. There are shown two different stellarator configurations with quasi-isodynamic symmetry and a stellarator with the maximum-$\mathcal{J}$ property, leading to a microstable type of turbulence.

1 Introduction

Nuclear fusion is a promising candidate as a future source of mass production of clean and safe energy. Nuclear fusion reactions are the main source of energy for stars, such as our Sun, and occur when two atomic nuclei combine to form a heavier atomic nucleus in addition to other products, namely neutrons and, most notably, energy. In order for a fusion reaction to take place, the nuclei need to overcome the large scale Coulomb force, due to their equal sign charges, so that they can be brought close enough together to be bound by the smaller scale attractive force between them. This process results in a modest decrease in mass, which in turn releases energy according to Einstein's famous formula $E = mc^2$.

A possible way known to harness this energy is by magnetic confinement of matter in which these reactions often take place - the plasma. Different magnetic confinement devices have been explored over several years with two toroidal configurations standing out: the tokamak and the stellarator, both invented in 1951.[1] In both devices the fusion confinement of the plasma is produced by a twisted toroidal magnetic field. However, in tokamaks this field is created by a toroidal plasma current whilst in stellarators it is produced by non-axisymetric coils, that is, they do not exhibit symmetry around an axis. Opposed to the stellarator, the tokamak is axisymmetric, thus confining all colisionless particle orbits, resulting in very good plasma confinement. Nonetheless, the necessary current can make them susceptible to current-driven instabilities and burdensome to operate in steady state. The stellarator's non-axisymmetry thus means that, in general, the plasma confinement is not as optimal, which can be mitigated by proper magnetic field optimization, but with the added value that the absence of current makes it intrinsically viable to operate in steady state.[2]

The production and development of these devices in an economically viable way has proven to be a very demanding endeavour, with countless factors that determine their performance. For the reactions to occur, the plasma must be confined at extremely high temperatures and densities for long timescales. Thus, it is crucial to have a magnetic field that best assures the conditions necessary for these processes to occur as well as optimal coils that are able to generate such field. One key aspect of the stellarator is that it has much more plasma flexibility in comparison to other devices, which while theoretically desirable, comes at the unwanted cost of increasing complexity in the coils. This characteristic leads to higher cost in the production of the physical devices questioning their economical viability. Hence, to diminish this problem, it is imperative to explore methods that can optimize the coil designs while also maintaining the performance of the plasma.[3]

Stellator optimizations are regularly performed computationally, although analytical approaches have been used (see Ref. [4]). Traditionally, stellarator optimization is accomplished with a two stage approach.[5] The first stage consists on obtaining the wanted properties of the target magnetic field equilibrium and the second focuses on finding a set of electromagnetic coils that can recreate such field. The second stage is, however, an ill-posed problem, because there are many possible coil configurations that can produce the same target field.[6] This can make it challenging to determine the optimal coil configuration for a given stellarator, because a slight modification in the plasma boundary may demand a significant adjustment to the coil geometry. Therefore, since the target magnetic field cannot

be changed, the coil design that is achieved as a product of the second stage of the optimization can be economically impracticable or even present an unrealistic challenge to the fabricator, due to the degree of complexity that it can reach. This would require another target field, leading to the restart of the process with the same uncertainty surrounding the viability of the coil production.

These challenges and difficulties may be resolved if a single-stage optimization approach is considered, in which the target magnetic field and its accompanying coils are varied at the same time. This way, there can be a balance between the plasma performance and the coil complexity, aiming to create a stellarator design with optimal confinement without creating an unrealistic engineering challenge for the electromagnetic coils.[3] This work expands on the recent preliminary results in vacuum obtained in Ref. [3]. Besides being only applicable in vacuum, Ref. [3] showed that there is still much room for improvement with regard to quasi-isodynamic stellarators (Section 2.3), since it was only found one configuration, for a single magnetic field period, that is far from optimal. Consequently, exploring this novel approach for quasi-isodynamic stellarator optimization is the primary goal of this project. In addition, it is also explored a desired stellarator property, known as maximum-$\mathcal{J}$, aiming to obtain a configuration that possesses it.

2 Materials and Methods

2.1 Governing equations

In order to guarantee a good design of a magnetic confinement device one obviously ought to take special care in the construction of the confining magnetic field. The goal of a tokamak or a stellarator is to confine a plasma with a certain pressure p by utilizing a magnetic field $\mathbf{B}$. This is possible due to the fact that the plasma has a current density, $\mathbf{J}$, that produces a magnetic force being able to balance the pressure force of the plasma.[2] Then, according to Ampère's law, in steady state, $\nabla \times \mathbf{B} = \mu_0 \mathbf{J}$, where the ponderomotive term has been neglected due to the fact that relativistic effects are not being considered.

Magnetic confinement fusion devices possess external coils that create most of the magnetic field. However, part of it is modified by the intrinsic plasma current. In order to achieve confinement, the necessary plasma current is given by the magnetohydrodynamic (MHD) equation of motion in steady state ($\partial_t = 0$) without plasma flows

$$\boldsymbol{J} \times \boldsymbol{B} = \nabla p. \tag{1}$$

From this equation follows that both $\boldsymbol{B}$ and $\boldsymbol{J}$ lie in surfaces of constant pressure, since both are perpendicular to the pressure gradient

$$\boldsymbol{J} \cdot \nabla p = \boldsymbol{B} \cdot \nabla p = 0. \tag{2}$$

Poincaré index (hairy ball) theorem states that a compact surface tangential to a non-vanishing vector field without any singularities must have the topology of a torus.[2, 7, 8] Nevertheless, even though it would be desirable, a purely toroidal magnetic field, on its own, is not able to supply sufficient confinement due to the resulting vertical drifts imparted to the particles. Hence, arises the need to add a poloidal component that is able to eliminate these. In essence this creates a helical field which can be generated by eletromagnetic coils in the case of the stellarator.[1]

Now it rises the question of how the stellarator is able to produce a helical magnetic field without a current running through the plasma to generate a poloidal twist. This so-called twist is normally represented by the rotational transform (ι), which globally indicates how many poloidal turns a certain field line makes during each toroidal turn around a surface of constant pressure, know as a flux surface.[2] At lowest order in the distance to the axis, the rotational transform can be written as

$$\iota = \frac{1}{2\pi} \int_0^L \left[\frac{\mu_0 J_\parallel}{2B} - (\cosh\eta - 1) d' - \tau \right] \frac{dl}{\cosh\eta} - N, \tag{3}$$

with $J_{\parallel} = \boldsymbol{J} \cdot \boldsymbol{B}/B$, η the elongation of the flux surface, d the angle of rotation of the surface as a function of the distance along the axis l and τ the axis torsion. This representation tells us that there are several ways of producing a rotational transform. The first term of the integral contributes to ι with a parallel plasma current, which is how the poloidal magnetic field is produced in the tokamak. The other terms are, respectively, the rotation of the poloidal cross-section of a flux surface when going around the torus in the toroidal direction and the torsion of the magnetic axis which is the innermost flux surface, that turns out to be just a line. These methods require breaking axisymmetry and are therefore usually used on stellarators.

In plasma confinement the best-case scenario is when the flux surfaces are nested, meaning that they lie inside each other. One useful way to describe this is by using magnetic coordinates, in which a particular coordinate remains constant on the surfaces that have a constant pressure, leading to the simplification of $\mathbf{B}$ on the coordinate system by using Eq. (2), and the field lines are straight in relation to the other coordinates.[2,9] This way, there is a certain coordinate choice that will be used from now on, the Boozer coordinates, where $\mathbf{B}$ becomes $\boldsymbol{B} = \nabla\psi \times \nabla\theta + \iota\nabla\varphi \times \nabla\psi = I(\psi)\nabla\theta + G(\psi)\nabla\varphi + \beta(\psi,\theta,\varphi)\nabla\psi$, with ψ being the coordinate that is constant in the flux surfaces, θ the poloidal angle, φ the toroidal angle, G the poloidal current, I the toroidal current and β a function proportional to the amount of pressure in the plasma.

2.2 Codes used

The main code used for the single-stage optimization process uses several different methods to obtain stellarator configurations, being able to perform the traditional two stage approach and also the novel single-stage one. It is open source and available in a github repository.[10]

In this single-stage process, a target magnetic field and the coils that produce it are varied simultaneously. The magnetic field equilibrium is obtained using the Variational Moments Equilibrium Code (VMEC)[11] that solves Eq. (1). The eletromagnetic coils are optimized using the SIMSOPT software.[12] These codes are now described in detail.

VMEC assumes a toroidal equilibrium with nested flux surfaces, using the steepest descent method [11] to find a minimum in the potential energy W resulting from an integral formulation of Eq. (1)

$$W = \int \left(\frac{|B|^2}{2\mu_0} + \frac{p}{\Gamma - 1} \right) dV, \tag{4}$$

with $\Gamma = 5/3$ being the ratio of specific heats and V the integration volume.[3] In this work, VMEC is ran in fixed boundary mode where the boundary flux surface S is fixed. Its coordinates are given by Fourier series ($S = [R(\vartheta,\phi)\cos(\phi), R(\vartheta,\phi)\sin(\phi), Z(\vartheta,\phi)]$) being specified in a cylindrical coordinate system by their Fourier amplitudes $\{\mathrm{RBC}_{m,n}, \mathrm{ZBS}_{m,n}\}$

$$R(\vartheta,\phi) = \sum_{m=0}^{M_{\mathrm{pol}}} \sum_{n=-N_{\mathrm{tor}}}^{N_{\mathrm{tor}}} \mathrm{RBC}_{m,n} \cos(m\vartheta - n_{\mathrm{fp}} n\phi), \tag{5}$$

and $Z(\vartheta,\phi)$ is similar with $\mathrm{ZBS}_{m,n}$ as coefficients and a sin function, where ϕ is the standard cylindrical angle, ϑ is a poloidal angle, and n_{fp} is the number of toroidal field periods of the magnetic field equilibrium.[3] An important property of S is its aspect ratio, which is related to the stellarator's volume in the sense that it is the quocient between the stellarator's major radius, which in this work is fixed as 1, and the minor radius, which is varied during the optimization.

In this process, each coil $\boldsymbol{\Gamma}^{(i)}$ is modeled as a closed, smooth curve in three dimensional space, represented by a periodic function and depicted as a Fourier series truncated at a number of N_F terms, namely[13,14]

$$\boldsymbol{\Gamma}^{(i)} = [\Gamma_1^{(i)}, \Gamma_2^{(i)}, \Gamma_3^{(i)}] : [0, 2\pi) \to \mathbb{R}^3, \tag{6}$$

where

$$\Gamma_j^{(i)} = c_{j,0}^{(i)} + \sum_{l=1}^{N_F} \left[c_{j,l}^{(i)} \cos(l\theta) + s_{j,l}^{(i)} \sin(l\theta) \right]. \tag{7}$$

This representation yields $3(2N_F + 1)$ degrees of freedom per coil.

In stellarators, a certain kind of symmetry, generally called stellarator symmetry, is usually imposed to reduce in half the number of coils and surface modes that one has to optimize. In a cylindrical coordinate system this can be expressed as $\psi(R, \phi, Z) = \psi(R, -\phi, -Z)$. An n_{fp} rotational symmetry is also imposed, with $\psi(R, \phi, Z) = \psi(R, \phi + 2\pi/n_{\text{fp}}, Z)$. One then places N_C independent coils encircling half of a field period, as the remaining ones can be found by performing simple transformations of the independent coils according to the symmetries, bringing the total number to $2n_{\text{fp}}N_C$.

The previously mentioned coil representation treats these as current-carrying filaments (the thickness of the coils is neglected).[3] The goal is to reproduce the equilibrium target magnetic field with the coils. The created field is evaluated using the Biot-Savart law

$$\mathbf{B}_{\text{ext}}(\bar{\mathbf{x}}) = \frac{\mu_0}{4\pi} \sum_{i=1}^{2n_{\text{fp}}N_C} I^{(i)} \int_{\mathbf{\Gamma}^{(i)}} \frac{d\mathbf{l}^{(i)} \times \mathbf{r}}{r^3}, \tag{8}$$

where $I^{(i)}$ is the current in the ith coil $\mathbf{\Gamma}^{(i)}$, $d\mathbf{l}^{(i)} = \mathbf{x}_i' d\theta$ is the differential line element, θ is an angle-like coordinate that parametrizes the coil curve (not to be confused with the stellarator's poloidal angle) and $\mathbf{r} = \bar{\mathbf{x}} - \mathbf{x}_i$ is the displacement vector between the evaluated point on the surface and the differential element. Thus, the degrees of freedom for the coil shapes are $\mathbf{x}_{\text{coils}} = [c_{j,l}^{(i)}, s_{j,l}^{(i)}, I^{(i)}]$.

In order to find appropriate coils, $\mathbf{x}_{\text{coils}}$ are varied to minimize the field error, which is simply the magnitude of the normal component of the magnetic field induced by the coils on the boundary surface.[14] This approach, usually termed FOCUS-like optimization (Ref. [14]), has already produced excellent results allowing for simple coil shapes with very low field errors.[13, 15] This minimization is accomplished by using the quadratic flux, f_{QF}, as a cost function, where f_{QF} is given by

$$f_{\text{QF}} = \int_S \left(\frac{\mathbf{B}_{\text{ext}} \cdot \mathbf{n}}{|\mathbf{B}_{\text{ext}}|} \right)^2 dS, \tag{9}$$

with $\mathbf{B}_{\text{ext}} = \mathbf{B}_{\text{ext}}(\mathbf{x}_{\text{coils}})$ and $\mathbf{n} = \mathbf{n}(S)$ is the boundary surface unit vector. The ultimate objective is to obtain $f_{\text{QF}} = 0$, which would mean that the field produced by the coils was perfectly matching the target magnetic field. However, as previously mentioned in Section 1, the electromagnetic coils problem is an ill-posed one. Due to this, it becomes imperative to limit the possible coil shapes by introducing penalties related to the coil complexity using the method described in Ref. [13]. Hence, regularization terms are imposed, such as a maximum length for each coil, a maximum curvature and a minimum distance between adjacent coils. These are all added to f_{QF} creating what is called an objective function, which one wants to minimize as much as possible in order to obtain the most optimal coil configuration.

2.3 Omnigenity and Maximum-$\mathcal{J}$ configurations

As mentioned in Section 1, the stellarator has a non-axisymmetric magnetic field which in general leads to inferior confinement of trapped particle orbits and does not guarantee the existence of nested magnetic flux surfaces.[16] Unrestricted paths of orbiting particles may create a significant issue in a reactor setting. This is due to the fact that the uncontrolled movement of energetic alpha particles can result in collisions with the first wall before thermalizing, causing harm to the components that face the plasma, which is not tolerable. Therefore, one key aspect regarding the optimization of stellarator devices during recent years has been the quality of particle confinement, where the sought out limit where every collisionless trajectory is confined is known as omnigenity. More accurately, omnigenity means that the radial guiding-center drift velocity averages to zero over time for all particles, with the

drift velocity being given by $\boldsymbol{v_d} = v_\parallel^2 \boldsymbol{B} \times \boldsymbol{\kappa}/(\Omega B) + v_\perp^2 (\boldsymbol{B} \times \nabla B)/(2\Omega B^2)$, where $v_\parallel$ and $v_\perp$ are the parallel and perpendicular components of the particle's velocity to the magnetic field line, $\boldsymbol{\kappa} = \boldsymbol{b} \cdot \boldsymbol{\nabla b}$, $\boldsymbol{b} = \boldsymbol{B}/B$, with $B = |\boldsymbol{B}|$ and $\Omega = ZeB/mc$ is the gyrofrequency, where Z is the species charge in units of the proton charge e, c is the speed of light and m is the particle's mass.[17] It is worth noting that there are also other equivalent definitions of omnigenity, such as the one in Ref. [18].

One way of obtaining omnigenity is via quasi-symmetry. A magnetic field is defined as quasi-symmetric if there exists an invariant direction for B in Boozer coordinates.[2, 13] This will lead to conservation of canonical angular momentum, which means that $P = -q\psi + mv_\parallel G/B$ is constant, where q is particle's charge and G is the poloidal current. A particle's drift is represented as $\Delta\psi$ and in this case is just $h\Delta(v_\parallel G/B)$, with $h = m/q$ being constant. The poloidal gyroradius is proportional to $mv_\parallel G/qB$ and so, the conservation of angular momentum guarantees that the drift away from a given flux surface is only on the order of the poloidal gyroradius, which implies omnigenity.[17] This can also be expressed as B varying on a surface of constant pressure only through a fixed linear combination of the toroidal and poloidal angles defined in Boozer coordinates, $B = B(\psi, M\theta - N\varphi)$, where the coefficients M and N are integers. If $N = 0$ the stellarator is said to have quasi-axisymmetry (QA) and if $N \neq 0$ it has quasi-helical symmetry (QH).

Another form of omnigenity is given by quasi-isodynamic (QI) stellarators, the main focus of this project. For an ideal perfectly constructed QI magnetic field with n_{fp} field periods one has to satisfy $\int (\boldsymbol{v_d} \cdot \boldsymbol{n}) dt = 0$ with poloidally closed contours of B. The difference between QI and quasi-symmetry is simply because in the latter all contours of B must be straight lines as opposed to only the ones of maximum B. Furthermore, in QH, the contours close helically, whilst in QA they close toroidally. If the B contours are straight and also close in the poloidal direction rather than toroidally, the field has quasi-poloidal symmetry, which is impossible to obtain next to the magnetic axis and has proven to be very arduous to find during optimization. Thus, as the conditions are much less strict for QI, it could be a favourable alternative.[18] The currently larger stellarator in operation, the Wendelstein 7-X (Greifswald, Germany), possesses approximate QI symmetry.[19]

Another way of defining omnigenity is through the parallel adiabatic invariant ($\mathcal{J}$). If a particle is unable to enter areas with magnetic field strength $B \geq B_{lim}$ it is defined as trapped and thus it will move along some fieldline between points l_1 and l_2 where the magnetic field strength is B_{lim}. In this scenario, the particle's $\mathcal{J}$ can be written as[18]

$$\mathcal{J} = \int_{l_1}^{l_2} mv_\parallel \, dl \,, \tag{10}$$

where m is the particle's mass and l is the geometric length along that field line. In the absence of an eletric field, for a particle with a constant Hamiltonian $\mathcal{H} = mv^2/2$, $v_\parallel$ is given by $\pm\sqrt{2\mathcal{H}/m}\sqrt{1 - \mu B/\mathcal{H}}$, with $\mu = mv_\perp^2/2B$ being another invariant of the particle's motion.

Due to the fact that $v_\parallel = 0$ when $B = B_{lim}$, and since $\mathcal{H}$, μ and m are constant for collisionless particles, $\mathcal{J}$ can be written as $\sqrt{2\mathcal{H}m}\int_{l_1}^{l_2}\sqrt{1 - \lambda B}\, dl$, with $\lambda \equiv 1/B_{lim} = \mu/\mathcal{H}$. In a perfect omnigenous field, $\partial\mathcal{J}/\partial\alpha|_{\psi,\lambda} = 0, \forall\psi, \lambda, \alpha$, where $\alpha = \theta - \iota\varphi$ is constant along the magnetic field and usually termed a field line label. The maximum-$\mathcal{J}$ property of a field is such that $\mathcal{J}$ decreases as a function of ψ, which is simply $\partial_\psi\mathcal{J} < 0$, turning out to be desirable in stellarators because it minimizes trapped-particle instabilities, resulting in a better performance. The reason behind this stems from the fact that if one were to consider a plasma instability that moves a particle radially outwards by $\Delta\psi$, that process would in fact cost energy if $\partial_\psi\mathcal{J} < 0$, not being as likely to occur. Therefore, the maximum-$\mathcal{J}$ property is beneficial for stability. This concept is thoroughly explained in Refs. [20, 21].

In order to obtain stellarators with this property, a code was developed to calculate $\mathcal{J}$ and its derivative given an input VMEC file, containing the characteristics of the plasma. This code was later included in the single-stage optimization code as a way to perform optimizations targeting this maximum-$\mathcal{J}$ property. The available surfaces in the file are finite, which means that the plasma does

not have a continuous description in the ψ coordinate, making it impossible to calculate a reliable numerical derivative. Due to this, for every configuration, an interpolation is made in this coordinate with the available surfaces, in order to calculate the derivative. The code calculates, for a given flux surface, the points where $v_{\parallel} = 0$, called turning points, to set the limits for the subsequent calculation of $\mathcal{J}$ using Eq. (10). Then, the process is repeated for a flux surface at a small distance ε away from the original surface, so that the two values of $\mathcal{J}$ can be used to calculate the numerical derivative.

3 Results

Henceforth are shown the results using the single-stage optimization approach to obtain a fixed boundary equilibrium that accurately reproduces the magnetic field created by the external coils and that minimizes an overall objective function. This approach helped obtain two quasi-isodynamic stellarators and a configuration with the maximum-$\mathcal{J}$ property. The objective function is the result of the weighted sum of the second stage objective function, discussed in Section 2.2, and the stage 1 objective, which takes into account how close a configuration is to quasi-symmetry or quasi-isodynamicity and to the target aspect ratio and, in the case of maximum-$\mathcal{J}$ optimizations, how close it is to a target for $\partial_{\psi}\mathcal{J}$.

All the results in this work are obtained in vacuum fields, making it possible to use Poincaré plots to verify the accuracy and consistency of the results. These plots are merely cross-sections of the magnetic field lines obtained using the magnetic field from the resulting coils, with the Biot-Savart law. To verify that the fixed boundary equilibrium obtained reproduces the magnetic field from the coils, a quadratic flux minimizing surface, or QFM, is created from the resulting coils and is compared to the original equilibrium. These are surfaces that minimize

$$f(S) = \frac{\int_0^{2\pi}\int_0^{2\pi/n_{\mathrm{fp}}}(\mathbf{B}\cdot\mathbf{n})^2 d\theta d\varphi}{\int_0^{2\pi}\int_0^{2\pi/n_{\mathrm{fp}}} B^2 d\theta d\varphi} + \frac{1}{2}[\mathrm{Vol}(\mathrm{QFM}) - \mathrm{Vol}(S)]^2, \tag{11}$$

having no constraints on the angles that parametrize the surface, with Vol(S) being the volume within the fixed boundary surface S and Vol(QFM) the volume within the QFM surface.[3] In the final part of the verification process, the fixed boundary and QFM surfaces are both compared simultaneously with the Poicaré plots. One aims to obtain a configuration where all 3 of these plots coincide.

Firstly, it is shown the optimization of two quasi-isodynamic stellarators with one field period and an aspect ratio of 7.0. In a stellarator, the higher the minor radius the more plasma there is, allowing for more particles and more collisions, making it more efficient to harness energy. With this in mind, it would be beneficial for the aspect ratio to be as low as possible. However, during preliminary optimizations, it was notable that lowering the aspect ratio meant that it was significantly more arduous to obtain a better quasi-isodynamic configuration. Generally, lowering the aspect ratio tends to make it more difficult to achieve better quasi-symmetry, as it can be seen in Fig. 4.

In order to obtain these configurations, it was used a set of 8 independent coils with a total of 16 Fourier modes (N_F), where the only difference between configurations was the maximum length used for each coil. The values chosen were 5.5 and 7.0, both with a minimum distance between coils of 0.12. For the results of the single-stage optimization with maximum length 5.5, the same length used in Ref. [3], the total objective was 5.8×10^{-3} and the total squared flux (see Eq. (9)) was 4.2×10^{-7}, with an average value of $\boldsymbol{B} \cdot \boldsymbol{n}$ of 8.3×10^{-5}. The results can be seen in Fig. 1. For the maximum coil length of 7.0 the results are shown in Fig. 2. The final total objective was 7.4×10^{-3} and the total squared flux was 3.0×10^{-7}, with an average value of $\boldsymbol{B} \cdot \boldsymbol{n}$ of 1.0×10^{-4}. The Poincaré plots, the fixed boundary and QFM surfaces are all also shown for each configuration, as well as the contours of constant magnetic field strength in Boozer coordinates. As it is clear from Fig. 2, the Poincaré plots do not agree with the QFM surfaces and the final equilibrium at the boundary, revealing the importance of not only comparing the results with the QFM surfaces but also always with the Poincaré plots.

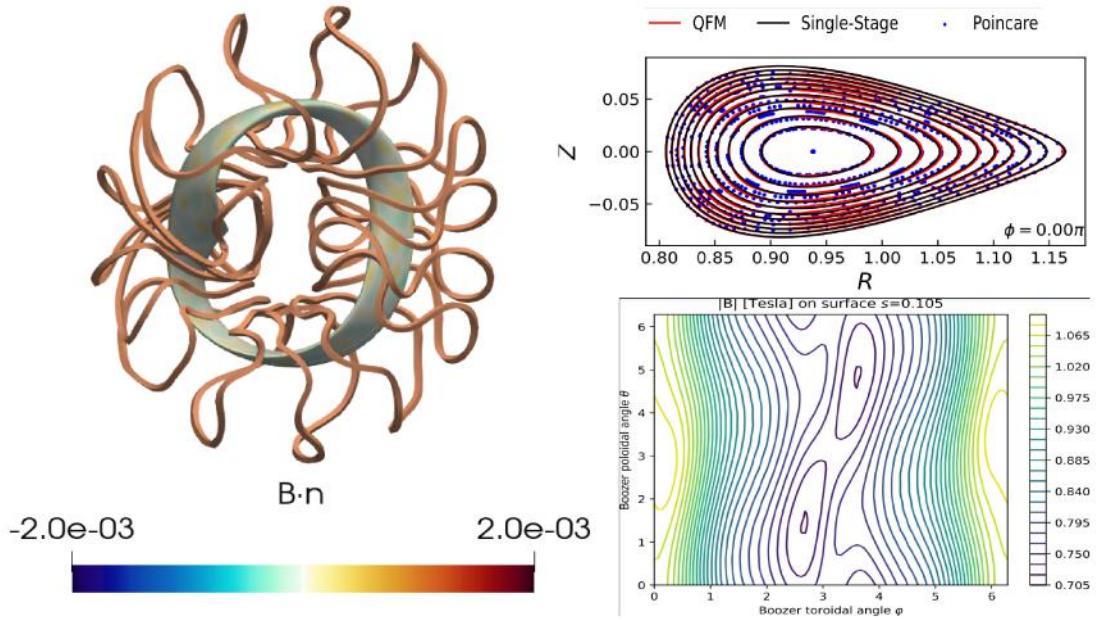

FIGURE 1: QI stellarator with 5.5 maximum length for each coil. Left: result of the single-stage optimization. Upper Right: superposition of the Poincaré plots, the QFM surfaces and final equilibrium. Lower Right: contours of constant magnetic field strength on a surface at $s = 0.105$ in Boozer coordinates.

Additionally, it is shown the optimization of a stellarator which has the maximum-$\mathcal{J}$ property (Fig. 3). To confirm this, several derivatives were calculated for different values of λ in the surfaces at $s = \psi/\psi_b = 5/16$ and $s = 10/16$, with ψ_b being the value of the ψ Boozer coordinate at the boundary, which were all lower than -0.15. The quasi-symmetry residuals from the stage 1 objective were 0.18, whereas the total final objective was 15. The final squared flux was 1.6×10^{-4} with an average value of $\boldsymbol{B} \cdot \boldsymbol{n}$ of 1.7×10^{-3}.

4 Conclusions and next steps

From the QI configurations found it is clear that this single-stage optimization method is very effective. Comparing the results of the 5.5 maximum length configuration to the ones obtained in Ref. [3] there was a slight improvement in the squared flux, which was previously 4.4×10^{-7}. The QFM surfaces also line up perfectly with the single-stage final equilibrium, showing an agreement with the Poincaré plots. In the second configuration, despite having a lower squared flux, the QFM surfaces show a higher deviation from the final equilibrium. However, there still is an agreement with these and the Poincaré plots along most of the volume surface, with some outliers in the boundary as previously mentioned, which seem to appear frequently in QI optimizations, even for larger coils. It is clear from the obtained configurations that the second one has much more complex coils, which was expected given that increasing the maximum length also increases the freedom of the coil shape. The first one seems to have much simpler coils, appearing possible to recreate physically. Finally, both displays of the contours of constant magnetic field strength show the QI character of the configurations.

The maximum-$\mathcal{J}$ configuration obtained is clearly not optimal. From the images it is evident that the field produced by the coils matches much more poorly with the target magnetic field in comparison with the QI configurations. The single-stage optimization was run to achieve a QA stellarator, however, from the resulting quasi-symmetry residuals and the contours of constant magnetic field

strength, one can understand that the result does not possess quasi-symmetry when compared to the existing optimized stellarators of this type (see Ref. [3]). Nevertheless, this result shows that the developed maximum-$\mathcal{J}$ code is able to obtain turbulence-optimized configurations.

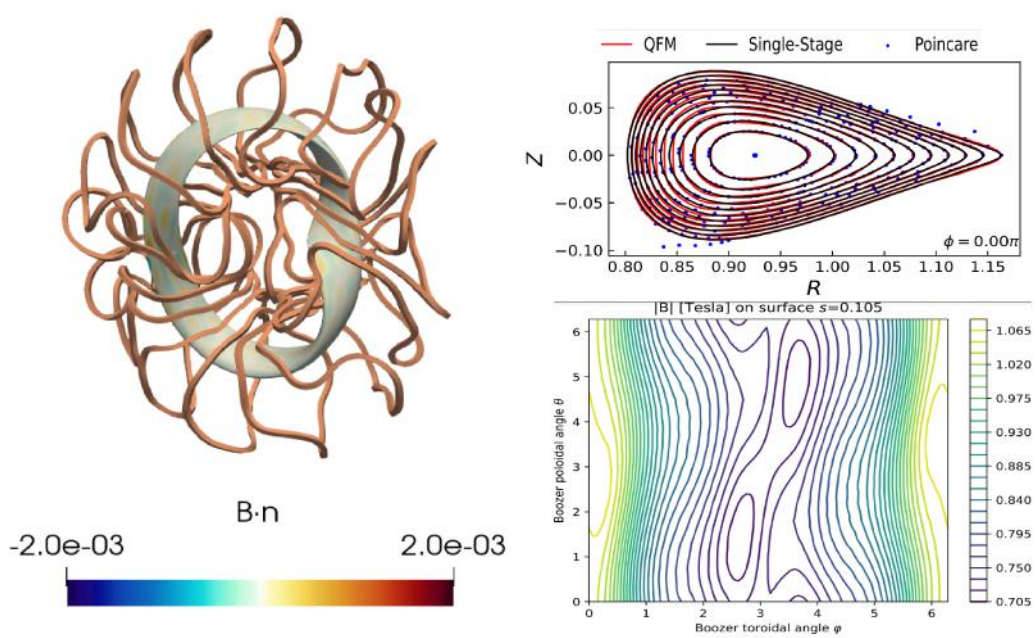

FIGURE 2: QI stellarator with 7.0 maximum length for each coil. Left: result of the single-stage optimization. Upper Right: superposition of the Poincaré plots, the QFM surfaces and final equilibrium. Lower Right: contours of constant magnetic field strength on a surface at $s = 0.105$ in Boozer coordinates.

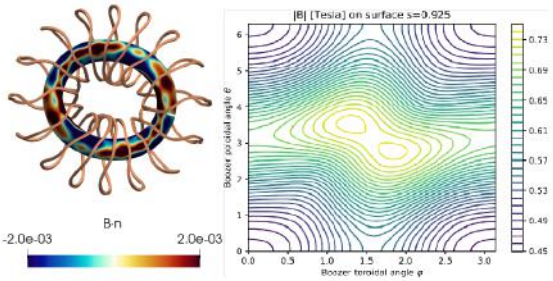

FIGURE 3: Maximum-$\mathcal{J}$ Stellarator with 5.4 maximum length for each coil and 0.17 separation between coils. Left: result of the single-stage optimization. Right: contours of constant magnetic field strength on a surface at $s = 0.925$ in Boozer coordinates.

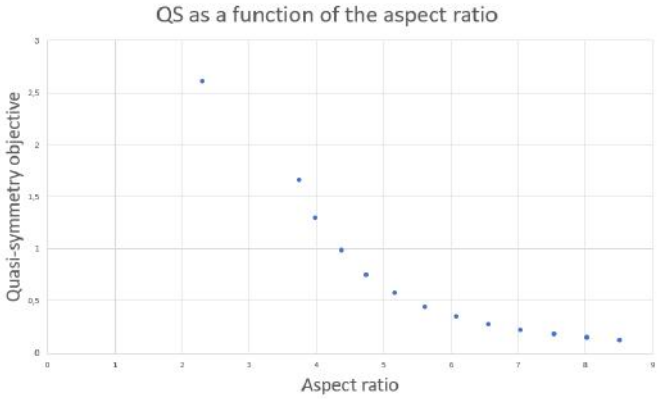

FIGURE 4: Quasi-symmetry objective for different aspect ratios after 20 iterations of a stage 1 optimization of a QH stellarator.

A natural next step would be to possibly understand the erratic behaviour of the Poincaré plots near the boundary for some QI configurations, attemping to obtain even better stellarators. For the maximum-$\mathcal{J}$ property it would be interesting to try to obtain one configuration with good quasi-axisymmetry or quasi-helical symmetry or, alternatively, prove theoretically that those are impossible to achieve, since it is conjectured that only QI stellarators can be maximum-$\mathcal{J}$. It would also be interesting to upgrade the single-stage optimization code to include finite plasma pressure optimizations

and also to discard optimizations where the coils intercept each other, given that those configurations are impossible to recreate in the real world.

References

[1] L.-M. Imbert-Gerard et al. "An Introduction to Stellarators: From magnetic fields to symmetries and optimization". In: *arXiv:1908.05360* preprint (physics.plasm-ph 2019).

[2] P. Helander. "Theory of plasma confinement in non-axisymmetric magnetic fields". In: *Reports on Progress in Physics* 77 (8 2014), p. 87001.

[3] R. Jorge et al. "Single-Stage Stellarator Optimization: Combining Coils with Fixed Boundary Equilibria". In: *Plasma Physics and Controlled Fusion* 65 (7 2023), p. 074003.

[4] R. Jorge et al. "Construction of quasisymmetric stellarators using a direct coordinate approach". In: *Nuclear Fusion* 60 (7 2020), p. 76021.

[5] B. E. Nelson et al. "Design of the national compact stellarator experiment (NCSX)". In: *Fusion Engineering and Design* 66-68 (2003), pp. 169–174.

[6] M. Landreman. "An improved current potential method for fast computation of stellarator coil shapes". In: *Nuclear Fusion* 57 (4 2017), p. 046003.

[7] W. P. Thurston. *Three-Dimensional Geometry and Topology, Volume 1*. Princeton, NJ: Princeton University Press, 1997.

[8] M. Eisenberg et al. "A Proof of the Hairy Ball Theorem". In: *The American Mathematical Monthly* 86 (7 1979), pp. 571–574.

[9] M. D. Kruskal et al. "Equilibrium of a Magnetically Confined Plasma in a Toroid". In: *The Physics of Fluids* 1 (1958), p. 265.

[10] R. Jorge. *SSO*. Github repository at https://github.com/rogeriojorge/single_stage_optimization (2023).

[11] S. P. Hirshman et al. "Steepest-descent moment method for three-dimensional magnetohydrodynamic equilibria". In: *Physics of Fluids* 26 (12 1983), p. 3553.

[12] M. Landreman et al. "SIMSOPT: A flexible framework for stellarator optimization". In: *Journal of Open Source Software* 6 (65 2021), p. 3525.

[13] F. Wechsung et al. "Precise stellarator quasisymmetry can be achieved with electromagnetic coils". In: *Proceedings of the National Academy of Sciences of the United States of America* 119 (13 2022), p. 2202084119.

[14] C. Zhu et al. "New method to design stellarator coils without the winding surface". In: *Nuclear Fusion* 58 (1 2018), p. 016008.

[15] A. Giuliani et al. "Direct computation of magnetic surfaces in Boozer coordinates and coil optimization for quasisymmetry". In: *Journal of Plasma Physics* 88 (4 2022), p. 905880401.

[16] C. D. Beidler et al. "Demonstration of reduced neoclassical energy transport in Wendelstein 7-X". In: *Nature 2021 596:7871* 596 (7871 2021), pp. 221–226.

[17] M. Landreman et al. "Omnigenity as generalized quasisymmetry". In: *Physics of Plasmas* 19 (5 2012), p. 056103.

[18] A. Goodman et al. "Constructing precisely quasi-isodynamic magnetic fields". In: *arXiv:2211.09829* preprint (physics.plasm-ph 2022).

[19] R. Jorge et al. "A single-field-period quasi-isodynamic stellarator". In: *J. Plasma Phys* 88 (2022), p. 175880504.

[20] J. H.E. Proll et al. "Turbulence mitigation in maximum-J stellarators with electron-density gradient". In: *Journal of Plasma Physics* 88 (1 2022), p. 905880112.

[21] P. Helander et al. "Stellarator and tokamak plasmas: a comparison". In: *Plasma Physics and Controlled Fusion* 54 (12 2012), p. 124009.